DFT Study on the Selectivity of Complexation of Metal Cations with a Dioxadithia Crown Ether Ligand

Jacek Korchowiec,[†,*] Beata Korchowiec,[‡] Waldemar Priebe,[§] and Ewa Rogalska[||]

Department of Theoretical Chemistry and Department of Physical Chemistry and Electrochemistry, Faculty of Chemistry, Jagiellonian University, Ingardena 3, 30-060 Krakow, Poland, The University of Texas M. D. Anderson Cancer Center, Houston, Texas 77030, and Structure et Réactivité des Systèmes Moléculaires Complexes, BP 239, CNRS/Nancy Université, 54506 Vandoeuvre-lès-Nancy cedex, France

Received: July 25, 2008; Revised Manuscript Received: October 06, 2008

The interactions of a dioxadithia crown ether ligand with Li^+, Na^+, K^+, Mg^{2+}, Ca^{2+}, and Zn^{2+} cations were investigated using density functional theory (DFT) modeling. The modeling was undertaken to gain insight into the mechanism of the selective complexation of the mono- and dications observed with this ligand experimentally. Two types of conformationally different complexes were located with both mono- and dications. In the first conformer, the cation is bonded to the ether oxygens; in the second conformer, the cation is bonded to the alkoxy and suger oxygens. In general, the complexes formed with dications were found to be more stable than those with monocations, with the stability decreasing with the period number within a given periodic table group of elements. The highest stability was observed for the complexes formed with zinc. The complex formed with lithium was the most stable among those involving monovalent cations. The system interaction energy was decomposed into electrostatic (ES), polarization (P), charge-transfer (CT), exchange (EX), and geometry-deformation (DEF) contributions using the self-consistent charge and configuration method for subsystems (SCCCMS). The stabilizing energy components (ES, P, and CT) exhibit the same trend as the total interaction energy, whereas the destabilizing contributions (EX and DEF) exhibit the opposite trend. It was found that the main contributions responsible for stabilization of the dicationic systems are the P and ES energies; in the monocationic systems, the CT stabilization is equally important. The gas-phase preferences changed when the solvent effect was included. The dioxadithia crown ether ligand preserved its selectivity toward Zn^{2+}, but the selectivity sequence toward monovalent cations was reversed.

1. Introduction

Designing ligands for selective complexation is of great importance. The class of macrocycles called crown ethers[1,2] has a high ability to bind metal cations. Crown ethers are diverse heterocycles and, in their simplest form, are cyclic oligomers of dioxane.[3] By changing the size of the ring; the electrodonor atoms such as oxygen, nitrogen, sulfur, or phosphorus; and the substituents, the properties of the system can be easily adjusted. For example, incorporating chiral centers in a crown ether allows chiral recognition upon complexation.[4] In this way, simple enzyme-like catalysts can be developed. On the other hand, grafting long hydrophobic chains onto a crown ether allows self-organization of the macrocycles.[5] The relative ease of preparation of a broad range of derivatives makes crown ethers attractive targets for both theoretical and applied studies.[3,6−8] Indeed, because of their host−guest complexation and molecular recognition properties, crown ethers have proved useful in sensing,[9] switching,[10] phase-transfer catalysis,[11] extraction,[12] and chromatography.[13,14] Crown ethers have also been used as membrane-forming amphiphiles;[15] as biomimetic receptors;[16] and because of their ionophoretic properties, as model ion channels.[17] The selectivity of complexation in crown ethers is poorly understood. It has usually been interpreted in terms of the size of the crown ether's cavity and the size of the guest ion. This suggests that the most stable complexes would be formed by crown ethers and ions that match in size. On the other hand, it should be kept in mind that the stability of the complexes formed depends to a great extent on the nature of the electrodonor atoms present in the ligand. The choice of the donor atoms in the crown ethers can be understood in terms of the hard-and-soft-acids-and-bases (HSAB) principle of Pearson;[18,19] the hard and soft cations are stably complexed by hard and soft electrodonors, respectively.

Broad molecular mechanics (MM) studies on the stability of crown ether−cation complexes were performed by Hancock and Martell.[20] Based on these MM calculations, the authors analyzed the role of the steric strain in the formation of the complexes. They concluded that the most stable complexes correspond to the lowest steric strain. Because some effects are usually lost in classical MM force-field calculations, however, an extension beyond MM is required. Modeling of selected crown ethers and their complexes at an ab initio level of theory is available in the literature.[21−32] For example, the formation of 18-crown-6 complexes was analyzed by Baerends et al.[21] and Glendening and co-workers[22,23] in terms of various energy components. Different reactivity criteria, such as the Fukui function, hardness, local softness, and the molecular electrostatic potential were applied by Geerlings and co-workers[32] to study the relative stability of selected crown ether complexes. However, to the best of our knowledge, no exhaustive study on the first-principles

* Corresponding author. E-mail: korchow@chemia.uj.edu.pl. Telephone: +48 12 6632030. Fax: +48 12 6340515.
† Department of Theoretical Chemistry, Jagiellonian University.
‡ Department of Physical Chemistry and Electrochemistry, Jagiellonian University.
§ The University of Texas M. D. Anderson Cancer Center.
|| Nancy Université.

10.1021/jp8066052 CCC: $40.75
Published on Web 12/04/2008

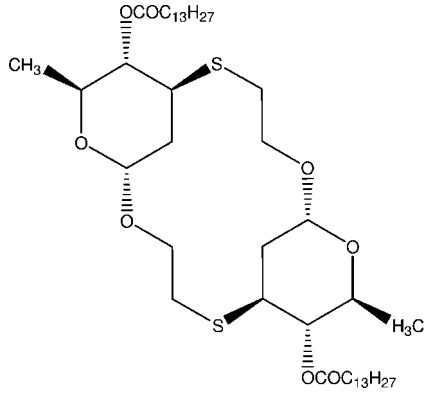

Figure 1. Structure of the dioxadithia crown ether ligand studied in this work.

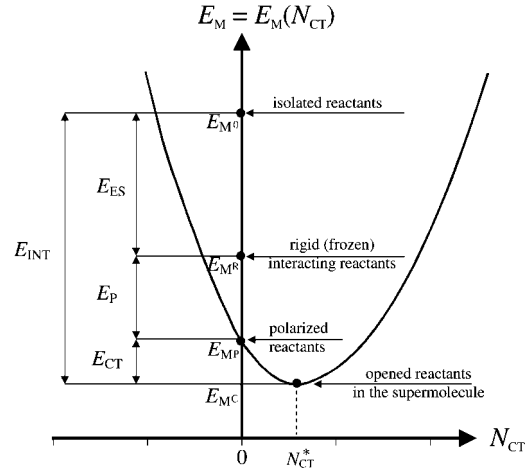

Figure 2. Qualitative cut of the energy surface in the population space $E_M = E_M(N_{CT})$ along the isoelectronic line $dq_A = -dq_B = N_{CT}$. The energies E_{M^0}, E_{M^R}, E_{M^P}, and E_{M^C} correspond to the system in the initial and intermediate stages of charge reorganization. The optimum amount of charge transfer is denoted as N^*_{CT}.

mechanism of the stability of the complexes formed with crown ethers is available.

In this article, we report the results of a DFT study of metal cation−crown ether complexes. The investigated ligand contains a hydrophilic 1,1′-dioxo-3,3′-dithio-14-crown ether headgroup and bears two myristoyl chains (Figure 1).

This amphiphilic molecule forms stable insoluble monolayers on the pure water surface and on various aqueous salt solution subphases. The physicochemical properties and metal complexing of these monolayers were studied in our previous work.[5] Here, we analyze the nature of the host−guest interactions between the 1,1′-dioxo-3,3′-dithio-14-crown ether ligand and Li^+, Na^+, K^+, Mg^{2+}, Ca^{2+}, and Zn^{2+} cations. The structure of these complexes was previously determined at the Hartree−Fock (HF)/6-31G level of theory.[5] The results of the modeling were in accordance with the differences between the compression isotherms corresponding to the mono- and dicationic systems. In this work, we focus on the nature of the interactions operating in these systems. The structures located in the preceding study were reoptimized at the density functional level of theory with an enlarged basis set. The interaction energy was decomposed into electrostatic, polarization, charge-transfer, exchange, and deformation contributions. Different energy partitioning schemes[33−43] and their extensions or modifications are described in the literature.[44−52] Here, the self-consistent charge and configuration method for subsystems (SCCCMS) was used.[43]

2. Computational Details

All calculations were carried out using the Gaussian 03[53] and GAMESS[54,55] suites of programs. The 6-31G* basis set[47] was adopted. A B3LYP[56] hybrid functional, i.e., a combination of the Becke's three-parameter exchange functional,[57] which partly includes the HF exchange, and the correlation functional of Lee, Yang, and Parr[58] were applied in the density functional calculations. A zigzag-type, all-trans conformation of the hydrocarbon chains was assumed. However, because of the rotational freedom, one can expect the existence of several other minima on the energy hypersurface, corresponding to the gauche conformation of selected parts of the hydrocarbon chain.

To characterize the investigated inclusion complexes, the interaction energy,

$$E_{int} = E_M - (E_A + E_B) \quad (1)$$

was decomposed using the self-consistent charge and configuration method for subsystems (SCCCMS). Here, E_M, E_A, and E_B denote the energies of the complex M and its two noninteracting subsystems A and B. The subsystems A and B are an acid (electron acceptor) and a base (electron donor), respectively. Within the polarization approximation (assumption of the SCCCMS scheme), the following hypothetical stages in the charge reorganization can be distinguished:[43] (i) separated (noninteracting) reactants, $M^0 = A^0 + B^0$; (ii) "rigid" (R) interacting reactants, $M^R = (A^0|B^0)$; (iii) polarized (P), mutually closed reactants (charge transfer between the reactants is not allowed), $M^P = (A^P|B^P)$; and (iv) mutually open reactants, $M^C = (A:B)$, in the complex. The solid and dotted lines between A and B represent mutually closed and open reactants, respectively. These stages are indicated in the plot shown in Figure 2. The energy surface is plotted along the isoelectronic line $dN_A = -dN_B \equiv N_{CT} > 0$, i.e., the direction in the population space preserving the total number of electrons in the system ($N_A + N_B$ = constant). Accordingly, one can distinguish the electrostatic (ES) $E_{ES} = E_{M^R} - E_{M^0}$, polarization (P) $E_P = E_{M^P} - E_{M^R}$, and charge-transfer (CT) $E_{CT} = E_{M^C} - E_{M^P}$ energy components. The CT contribution to the interaction energy can be derived by searching for the minimum of E_M with respect to N_{CT}. All of the distinguished components sum to give the interaction energy, E_{INT}. This energy term is different from that in eq 1 because of the assumed polarization approximation. The equivalence is possible upon addition of two additional components to E_{INT}, namely, the exchange-repulsion (EX) and geometry-deformation (DEF) components. The latter term, $E_{DEF} = (E^0_A + E^0_B) - (E_A + E_B)$, results from the fact that the geometries of the subsystems A and B in the supermolecule (with energies E^0_A and E^0_B) are different from those of the isolated reactants in the minimum-energy structures (with energies E_A and E_B). The former term results from the balance equation

$$E_{ES} + E_P + E_{CT} + E_{EX} + E_{DEF} = E_{INT} + E_{EX} + E_{DEF} = E_{int}$$

The negative or positive sign of a given contribution to the interaction energy indicates a stabilizing or destabilizing effect, respectively. The energetic requirements for each energy component are obvious based on their definitions. Correspondingly, the DEF and EX terms (the latter for closed-shell systems) must be positive, whereas the P and CT contributions must be negative; the electrostatic component can be either positive or negative.

In this work, SCCCMS calculations for four points of an isoelectronic line were performed. Specifically, the systems

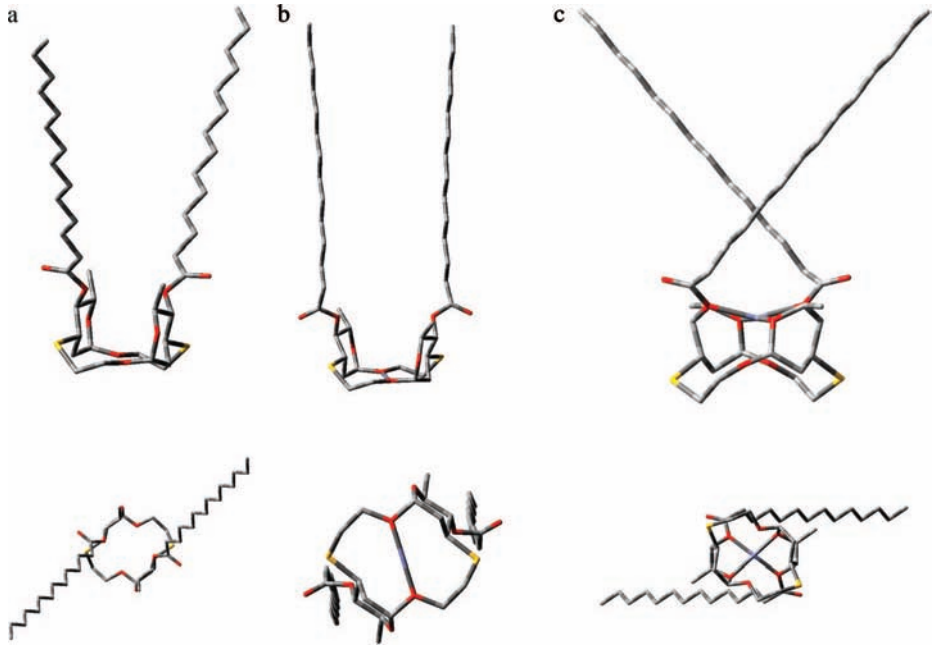

Figure 3. Side and top views of the geometrical structures of (a) the **CE** ligand and (b,c) its two conformationally different complexes with Zn^{2+}. Panels b and c correspond to the conformers 1 and 2, respectively. For clarity, the hydrogen atoms were omitted.

($M^{2+}|CE^{-}$), ($M^{+}|CE$), ($M|CE^{+}$), and ($M^{-}|CE^{2+}$) were considered for the complexes formed with alkali cations, and the systems ($M^{3+}|CE^{-}$), ($M^{2+}|CE$), ($M^{+}|CE^{+}$), and ($M|CE^{2+}$) were considered for the complexes of the divalent alkaline earth and zinc cations. The energy of each system was interpolated by a third-order Taylor expansion

$$E(N_{CT}) = E_0 + \mu_{CT}N_{CT} + \frac{1}{2}\eta_{CT}{N_{CT}}^2 + \frac{1}{6}\zeta_{CT}{N_{CT}}^3$$

where the CT quantities have the following definitions

$$\mu_{CT} = \left(\frac{\partial E}{\partial N_{CT}}\right) = \mu_A - \mu_B$$

$$\eta_{CT} = \left(\frac{\partial^2 E}{\partial {N_{CT}}^2}\right) = \eta_{AA} + \eta_{BB} - 2\eta_{AB}$$

and

$$\zeta_{CT} = \left(\frac{\partial^3 E}{\partial {N_{CT}}^3}\right) = \zeta_{AAA} + 3\zeta_{ABB} - \zeta_{BBB} - 3\zeta_{AAB}$$

The first-order responses

$$\mu_A = \left(\frac{\partial E}{\partial N_A}\right) \quad \text{and} \quad \mu_B = \left(\frac{\partial E}{\partial N_B}\right)$$

are the well-known chemical potentials of the reactants (negative electronegativities). The second-order derivatives are components of the hardness matrix $\boldsymbol{\eta}$

$$\eta_{AA} = \left(\frac{\partial^2 E}{\partial N_A \partial N_A}\right), \eta_{AB} = \left(\frac{\partial^2 E}{\partial N_A \partial N_B}\right), \text{ and } \eta_{BB} = \left(\frac{\partial^2 E}{\partial N_B \partial N_B}\right)$$

The third-order derivatives

$$\zeta_{AAA} = \left(\frac{\partial^3 E}{\partial N_A \partial N_A \partial N_A}\right), \zeta_{AAB} = \left(\frac{\partial^3 E}{\partial N_A \partial N_A \partial N_B}\right),$$

$$\zeta_{ABB} = \left(\frac{\partial^3 E}{\partial N_A \partial N_B \partial N_B}\right), \text{ and } \zeta_{BBB} = \left(\frac{\partial^3 E}{\partial N_B \partial N_B \partial N_B}\right)$$

are less known but should be taken into account for strongly interacting subsystems. All derivatives were computed for the constant external potential. The ($M^{+}|CE$) and ($M^{2+}|CE$) systems were used as references for the monovalent and divalent cations, respectively. The amount of CT was measured with respect to the reference system. The charge distribution inside the ether ligand was derived according to the Chirlian and Franci scheme.[59] The charge of the metal cation was held constant during a given SCCCMS run.

3. Results and Discussion

The investigated ligand contains a hydrophilic 1,1′-dioxo-3,3′-dithio-14-crown ether headgroup and two myristoyl chains (Figure 3a). For simplicity, the crown ether is denoted as CE. The sugar cycles are in the chair conformation. Two different coordination modes with cations yielding different conformations were identified. In the first mode, the sugar units are in the chair conformation, and the cation is coordinated by the two crown oxygen atoms (conformer 1). In the second mode, the sugar units are in the twisted-boat conformation, and the cation is located in a cage formed by four oxygens (conformer 2), two from the sugar cycle and two from the ester bond. The topologies of the two conformers are shown in Figure 3b,c, respectively.

The interaction energy, E_{int}, and its components, E_{ES}, E_P, E_{CT}, E_{EX}, and E_{DEF}, are collected in Table 1. All complexes are thermodynamically stable ($E_{int} < 0$), and the data reported in Table 1 fulfill the energetic requirements; the stabilizing P and CT contributions are negative, whereas EX and DEF are the positive destabilizing contributions. In all cases, the ES term is negative.

The stabilization decreases with increasing ionic radius (R): $E_{int}^{CE-Li^+} < E_{int}^{CE-Na^+} < E_{int}^{CE-K^+}$ and $E_{int}^{CE-Mg^{2+}} < E_{int}^{CE-Ca^{2+}}$ (R_{Li^+} = 0.76 Å, R_{Na^+} = 1.02 Å, R_{K^+} = 1.38 Å and $R_{Mg^{2+}}$ = 0.72 Å, $R_{Ca^{2+}}$ = 0.99 Å). The highest stabilization is observed with CE—Zn^{2+}. It should be noted that the ionic radius of Zn^{2+} ($R_{Zn^{2+}}$ = 0.74 Å) is close to that of Mg^{2+}. The complexes formed with divalent cations are more stable than those formed with monovalent cations. Except for CE—K^+, conformer 2 is more stable than conformer 1. The differences between the conformers are more significant with the divalent cations than with the

TABLE 1: Decomposition of the Interaction Energy (int) into Electrostatic (ES), Polarization (P), Charge-Transfer (CT), Exchange (EX), and Geometry-Deformation (DEF) Components[a]

complex	int	ES	P	CT	EX	DEF
			Conformer 1			
CE−Li^+	−62.4	−39.8	−50.2	−52.3	67.2	12.7
CE−Na^+	−35.7	−22.8	−30.8	−32.6	38.0	12.6
CE−K^+	−29.6	−12.6	−19.6	−23.5	21.6	4.5
CE−Mg^{2+}	−213.7	−88.8	−194.1	−73.1	114.5	27.7
CE−Ca^{2+}	−127.3	−54.1	−109.0	−45.0	64.7	16.2
CE−Zn^{2+}	−274.5	−100.5	−210.3	−61.0	63.7	33.7
			Conformer 2			
CE−Li^+	−66.3	−47.9	−45.8	−61.4	59.9	30.9
CE−Na^+	−48.4	−34.6	−32.4	−31.3	25.3	24.5
CE−K^+	−28.4	−25.5	−23.9	−11.4	8.2	24.1
CE−Mg^{2+}	−248.4	−125.1	−181.1	−73.6	75.2	56.2
CE−Ca^{2+}	−174.3	−93.1	−130.0	−30.5	33.6	45.7
CE−Zn^{2+}	−299.9	−129.3	−194.1	−87.6	57.6	53.5

[a] All values are in kcal mol^{-1}.

TABLE 2: Values of CIBO and CBO between the CE Oxygen Atom and the Cation (X) and the Corresponding Distances R_{O-X} for Conformer 1

CE−X	CIBO	CBO	R_{O-X} (Å)
CE−Li^+	0.487	0.260	1.845
CE−Na^+	0.357	0.200	2.255
CE−K^+	0.151	0.073	2.688
CE−Mg^{2+}	0.617	0.415	1.918
CE−Ca^{2+}	0.405	0.287	2.281
CE−Zn^{2+}	0.565	0.472	1.874

TABLE 3: CIBO and CBO between the CE Oxygen Atoms and the Cation (X) and the Corresponding Distances R_{O-X} for Conformer 2[a]

	CIBO		CBO		R_{O-X} (Å)	
CE−X	ester bond	sugar cycle	ester bond	sugar cycle	ester bond	sugar cycle
CE−Li^+	0.319	0.327	0.211	0.203	2.073	2.160
CE−Na^+	0.227	0.227	0.180	0.160	2.441	2.500
CE−K^+	0.117	0.100	0.121	0.093	2.880	2.871
CE−Mg^{2+}	0.408	0.438	0.337	0.304	2.119	2.155
CE−Ca^{2+}	0.235	0.239	0.205	0.195	2.529	2.537
CE−Zn^{2+}	0.384	0.379	0.353	0.312	2.037	2.084

[a] Columns 2, 4, and 6 correspond to the ester bond oxygens, and columns 3, 5 and 7 correspond to the sugar cycle oxygens.

monovalent cations. As for the interaction energy, each term of the energy partitioning is sensitive to the cation. The stabilizing contributions show a tendency consistent with that displayed by the interaction energies: $E_X^{CE-Li^+} < E_X^{CE-Na^+} < E_X^{CE-K^+}$ and $E_X^{CE-Mg^{2+}} < E_X^{CE-Ca^{2+}}$, where X = ES, P, and CT. The other two components exhibit an opposite tendency: $E_X^{CE-K^+} < E_X^{CE-Na^+} < E_X^{CE-Li^+}$ and $E_X^{CE-Ca^{2+}} < E_X^{CE-Mg^{2+}}$, where X = EX and DEF. However, such behavior does not invert the order observed for the stabilizing contributions. The components of the interaction energy for CE−Zn^{2+} are closer to those for CE−Mg^{2+} than to those for the other complexes for both coordination modes. This qualitative trend is consistent with the inter-reactant separations reported in Table 2, column 4, and Table 3, columns 6 and 7 (see also the bonds between the central ion and the ligand in Figure 3b,c). For example, the EX energy decreases with increasing inter-reactant separation as this contribution strongly depends on the mutual separation; the same is true for the DEF energy.

For the divalent cation complexes, the stabilizing contributions follow the order: $E_P^{CE-X^{2+}} < E_{ES}^{CE-X^{2+}} < E_{CT}^{CE-X^{2+}}$, X = Mg, Ca, and Zn. A similar behavior was reported for the complex of 18-crown-6 formed with Mg^{2+}.[23] However, for the 18-crown-6/Ca^{2+} system, the ES stabilization was slightly lower than the P stabilization. It should be noted that the complexes of 18-crown-6 are structurally close to conformer 1. The observed trends are similar; the P stabilization decreases much faster with increasing period number than the ES stabilization. This is particularly well seen with the monovalent cations. This behavior could be expected because it is linked to the increase of the electron density softness. A direct comparison of the two energy schemes is difficult. In our scheme, the restrictions are imposed on the electron density, whereas in natural energy decomposition analysis (NEDA),[40,41] they are imposed on the wave function. Therefore, the NEDA distortion (destabilizing) energies are mainly included in the exchange repulsion energy and, to a lesser degree, in the CT energy. In the case of CE−X^+ (X = Li, Na, K), the differences between the ES, P, and CT contributions are less pronounced, and the order depends on the coordination mode. For conformer 1, the highest stabilization comes from the CT energy, whereas the lowest is from the ES energy ($E_{CT}^{CE-X^{2+}} < E_P^{CE-X^{2+}} < E_{ES}^{CE-X^{2+}}$). Conformer 2 does not reveal any general regularity, except for the ES stabilization, which is always higher than the P stabilization. Here, direct reference to the NEDA data[22] is impossible because the first-order (ES) and second-order (P) electrostatic contributions were not further separated. As was the case with 18-crown-6, the CT energy is less important than the sum ES + P. For the monovalent cations, CT is 23−73% as strong as the whole electrostatic stabilization, and for the divalent cations, CT is 13−28% as strong as ES + P.

The fact that the difference $|E_P^{CE-X^{2+}} - E_{ES}^{CE-X^{2+}}|$ for X = Mg, Ca, and Zn is more pronounced than that observed with the monovalent cations can be easily explained. Indeed, a cation with a higher charge would have a greater impact on the reorganization of the electron density of the ligand. One should remember that in the computation of the ES term, the electron densities of both reactants were kept frozen. This explains why the second-order electrostatic contribution, that is, the polarization contribution (P), is more important in the case of divalent ions. For uncharged reactants, $|E_P|$ is smaller than $|E_{ES}|$,[60−62] as long as the assumption of polarization approximation is valid; otherwise, unphysical values are obtained.[44] The latter situation occurs with very short inter-reactant separations.

The charge reorganization pattern is reflected in the bond-order (BO) data listed in Tables 2 and 3. The BO parameters were calculated using two schemes. The first scheme takes into account only the covalent BO (CBO),[63−65] whereas the second scheme includes both covalent and ionic BO (CIBO) information.[66,67] In both tables, the BOs between the cation and the nearest oxygen atoms are listed together with the corresponding distances. For the first coordination mode, only one set of values is given, whereas for the second coordination mode, two sets are reported (Figure 3).

The two BO data sets are different. Except for CE−K^+, the CIBO parameters are greater than their CBO counterparts. The differences are more pronounced for conformer 1 than for conformer 2. This indicates a significant ionic contribution to the BOs. The BO data are consistent with the interaction energies for both conformers (Table 1). In other words, for a given conformer, a larger value of E_{int} corresponds to a larger BO index and to a shorter inter-reactant separation. The CIBO indexes for conformer 1 are always more important than those

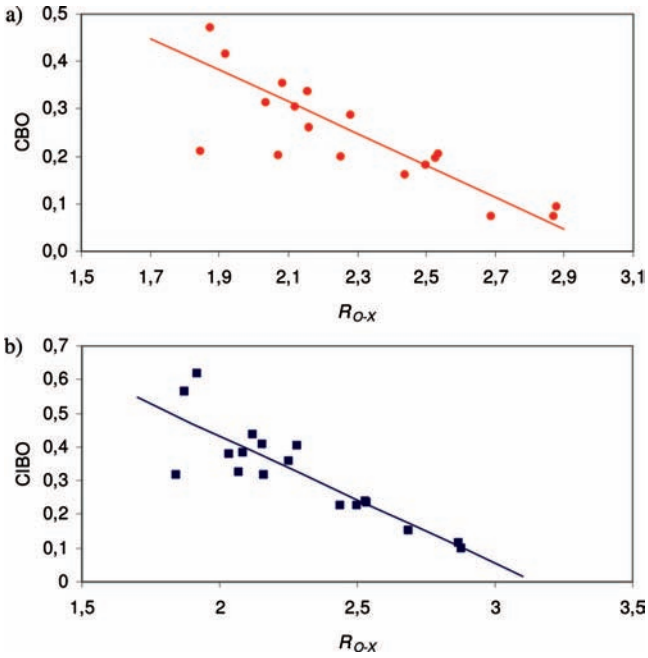

Figure 4. Dependence of (a) CBO and (b) CIBO on the R_{O-X} distance; $X = Li^+$, Na^+, K^+, Mg^{2+}, Ca^{2+}, and Zn^{2+}. The lines show the best linear approximations.

for conformer 2. This trend is in agreement with the inter-reactant separations. The distance between the cation and the CE oxygen in conformer 1 is always shorter than that in conformer 2. Nevertheless, it is not contradictory to the interaction energies, as only two equivalent oxygens make significant contributions to the CIBO in conformer 1 whereas two such sets of equivalent oxygen atoms exist in conformer 2.

The CBO data show the same tendency as the CIBO data, except for the CE—K^+ system. These results indicate a correlation between the R_{O-X} distance and the CIBO (and CBO) indexes (Figure 4). The linear correlation coefficients are 0.82 and 0.87 for the CBO and CIBO data, respectively. The correlation is even better when mono- and dications are considered separately.

It can be noticed that the obtained BO values are different from typical covalent bond-order data. Indeed, the C—H, C—C, C—O, and O—H bond orders are close to unity for both the CBO and CIBO schemes, as the ionic contribution differentiating the schemes is negligible. For example, the BO indexes for C—H bond in the CE—Zn^{2+} complexes are situated in the ranges of 0.989−1.030 and 0.891−1.000 within the CIBO and CBO schemes, respectively.

Steric and polar effects are frequently used when discussing the bond-forming and bond-breaking processes. However, these effects are intuitive. For example, Lefour et al.[68] identified the polar effect as the sum of ES, P, and CT contributions. On the other hand, Radom and co-workers[69−71] limited polar effects to only the CT component. One should also remember that the CT and ES components are closely related to the hard-and-soft-acids-and-bases (HSAB) principle of Pearson.[18,19] The strong affinity of a soft acid for a soft base is a CT-controlled process,[72] whereas the affinity of a hard acid for a hard base is an ES-controlled process.[73] Steric repulsion can be identified as the sum of the EX and DEF contributions, although different definitions are often used; for example, Lefour et al. identified the steric term exclusively with the EX contribution.[68] However, such effects as bond weakening, rehybridization, and resonance destabilization are naturally included in the DEF energy and

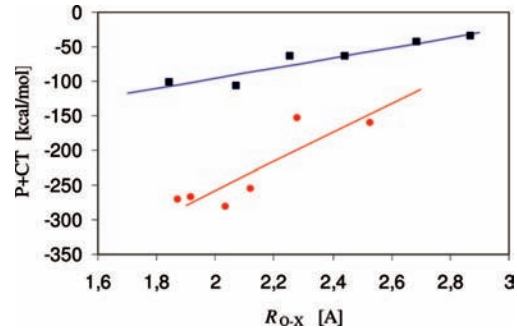

Figure 5. Relationship between the orbital energy (P + CT) and the inter-reactant separation. The squares and circles correspond to the mono- and dications, respectively. The lines illustrate the best linear approximations.

should be considered as steric effects, as argued by Tedder and Walton.[74−76] The other intuitive concepts used in the qualitative justifications of the observed trends in reactivity are orbital, Pauli, and electrostatic contributions. Here, the orbital energy is considered as the sum of the P and CT contributions.[37]

The data reported in Table 1 can be used to analyze these intuitive concepts. It can be seen that the polar effect (ES + P + CT) favors formation of conformer 2; the steric effect (EX + DEF) does not reveal such regularities. Indeed, the EX term favors conformer 2, whereas the DEF term favors conformer 1. The overall steric effect is a subtle interplay between the EX and DEF contributions. Therefore, the DEF destabilization reverses the general orientation rule only in the weakly bonded CE—K^+ complex, yielding a slightly more stable conformer 1.

In the CE—X^+ complexes, three energy contributions, namely, P, CT, and EX, show a linear correlation with R_{O-X}; the correlation coefficients are 0.93, 0.92, and 0.98, respectively. The other contributions do not show linear correlations. In the case of divalent cations, the correlation is still lower. Indeed, only the P and CT contributions show correlations higher than 0.75. The sum P + CT (the orbital contribution) has a relatively high linear correlation coefficient of 0.88. The better correlation of P + CT with distance for short inter-reactant separations is related to the fact that P + CT is less basis-set-dependent than the individual components.[51] The corresponding plot is shown in Figure 5. For the monovalent cations, the correlation between the P + CT energy and R_{O-X+} is 0.94. There is no linear correlation between the polar energy contribution and the distance, regardless of the definition used. There is no correlation for the steric repulsion either. These results are in agreement with the intuitive understanding of the interactions between chemical species. From this qualitative analysis, the following picture of interactions emerges: The ES term is responsible for the initial mutual orientation of reactants. The orbital (P + CT) energy, which is a strongly distance-dependent contribution, is the driving force for the formation of the complex. This term is also responsible for the electron density reorganization within the complex. Finally, the steric repulsion (EX + DEF) that reflects the local geometrical environment hinders bond formation.

To complete the energetic analysis of the interactions, the charge reorganization pattern has to be considered. The overall change in the electron density [$\Delta\rho(\vec{r}) = \rho_{M^C}(\vec{r}) - \rho_{M^R}(\vec{r})$] and its P [$\Delta\rho_P(\vec{r}) = \rho_{M^P}(\vec{r}) - \rho_{M^R}(\vec{r})$] and CT [$\Delta\rho_{CT}(\vec{r}) = \rho_{M^C}(\vec{r}) - \rho_{M^P}(\vec{r})$] components are plotted in Figure 6.[77] Because of the assumed polarization approximation, the CT density plot includes the EX reorganization. Here, it is termed CT. The blue isosurfaces (Figure 6) correspond to positive values (an increase in electron density), whereas the red isosurfaces correspond to

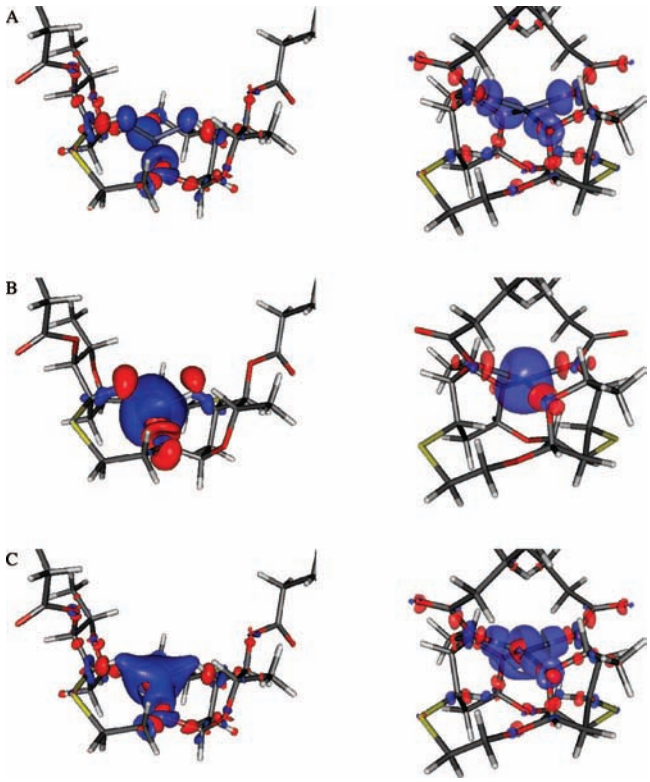

Figure 6. Charge reorganization plots for conformer 1 (left column) and conformer 2 (right column) of the CE—Zn^{2+} complex. Panels a—c correspond to $\Delta\rho_P(\vec{r})$, $\Delta\rho_{CT}(\vec{r})$, and $\Delta\rho(\vec{r})$, respectively. The positive and negative isosurfaces are denoted with blue and red, respectively. The value of the CT isosurface is |0.0025| au. The other values of isosurfaces are equal to |0.005| au.

negative values (a decrease in electron density). The figure illustrates both coordination modes for the CE—Zn^{2+} complex. The values of the isosurfaces are 0.0025 and 0.005 for $\Delta\rho_P(\vec{r})$ and$\Delta\rho_{CT}(\vec{r})$, respectively. The isosurface value of the $\Delta\rho(\vec{r})$ plot is the same as for $\Delta\rho_P(\vec{r})$. It can be seen that the P-related charge reorganization covers a significantly larger space than that related to CT. Whereas the CT plot includes the nearest neighborhood of the cation, the P plot extends to the crown and sugar cycle. The overall and P plots are qualitatively similar. During the P process, the electron density is concentrated in the nearest surroundings of Zn^{2+}. Part of this excess density is then transferred to the cation. Therefore, the isosurfaces of given atoms in the P and CT plots have different signs.

The charge reorganization plots are in accordance with the data reported in Table 1. The P contribution is a dominant term; it is approximately 3 and 2 times higher than the CT contribution for conformers 1 and 2, respectively. Therefore, the overall $\Delta\rho(\vec{r})$ plot resembles that of $\Delta\rho_P(\vec{r})$. The importance of the charge polarization, which enhances the electrostatic interactions, was also reported for 18-crown-6 complexes.[22,23]

The 1,1′-dioxo-3,3′-dithio-14-crown ether ligand with two myristoyl chains was designed as a potential ionophore. So far, its membrane-related properties have been studied in monomolecular films spread on pure water and on aqueous solutions of mono-, di-, and trivalent metal salts. The thermodynamic properties obtained from the monolayer experiments cannot be related to the single ether molecule or its complexes, because they describe the entire system. The only parameter that can be directly compared to the computed values is the limiting molecular areas per molecule. The molecular areas estimated with HF theory used in the previous study[5] explained fairly well the observed differences among the films obtained on pure water and on aqueous solutions of the mono- and divalent metal salts. These differences can be interpreted in terms of conformational changes occurring in the crown ether derivatives upon complexation. Taking into account the fact that crown ethers show pronounced selectivities, the latter point was investigated in this study as well.

The interaction energies indicate that binding of Zn^{2+} in CE is stronger than binding of the other dications. For the monocations, the CE—Li^+ complex is the preferred one. However, as was demonstrated for 18-crown-6 derivatives,[22,23] selectivity is not an intrinsic property of the crown ether itself. Indeed, the selectivity results from a competition between the solvent and the ether molecules for the cation. The exothermicity/endothermicity of the exchange reactions

$$\mathrm{CE{-}M^+ + Li^+(H_2O)_n \rightarrow CE{-}Li^+ + M^+(H_2O)_n} \quad n = 1, 2, 3, \text{or } 4 \quad (2)$$

$$\mathrm{CE{-}M^{2+} + Mg^{2+}(H_2O)_n \rightarrow CE{-}Mg^{2+} + M^{2+}(H_2O)_n} \quad n = 1, 2, \text{or } 6 \quad (3)$$

can be considered as an approximate measure of selectivity. It should be noted that these selectivity criteria involve only pure CE—M^{2+} and $M^{2+}(H_2O)_n$ complexes while omitting the mixed CE—$M^{2+}(H_2O)_m$ complexes. As was demonstrated by Glendening and co-workers for 18-crown-6 and alkali cations,[22,23] the mixed clusters did not influence the calculated selectivity trends while increasing the computational costs.

The exchange reaction enthalpies plotted as a function of the coordination number for mono- and dicationic systems are shown in Figure 7. All reaction enthalpies were computed at 298 K. Different water arrangements around the cations were taken into account. The lowest localized energy structure was used. Zero-point energies and enthalpy corrections were evaluated using standard statistical mechanical expressions. The B3LYP frequencies are unscaled. For a given hydration number n, the most exothermic (negative) reaction is the preferred one. The zero line in Figure 7a or b corresponds to the reference reaction CE—Li^+ + $Li^+(H_2O)_n$ → CE—Li^+ + $Li^+(H_2O)_n$ or CE—Mg^{2+} + $Mg^{2+}(H_2O)_n$ → CE—Mg^{2+} + $Mg^{2+}(H_2O)_n$, respectively. In the absence of the solvent molecules ($n = 0$), the previously obtained gas-phase, intrinsic CE selectivity rules toward mono- and dications are reproduced: $Li^+ > Na^+ > K^+$ and $Zn^{2+} > Mg^{2+} > Ca^{2+}$. It can be seen that the water molecules strongly influence the selectivity. The intrinsic sequence for monocations is reversed ($K^+ > Na^+ > Li^+$) for the highest degree of hydration. In the case of dication systems, the situation is slightly different. Indeed, the alkaline earth dications (Mg^{2+} and Ca^{2+}) change their order for $n > 3$, whereas the selectivity of Zn^{2+} is unchanged for the highest degree of hydration but is reversed for $n = 4$. Nevertheless, the difference between the exchange reaction enthalpies for the Ca^{2+} and Zn^{2+} systems is rather small. Such behavior of the zinc dication can be attributed to the 3d atomic orbitals.

Finally, we want to remark that the available kinetic and thermodynamic data for macrocycle ligand—cation systems were published by Izatt et al. in different reviews.[6,7,78,79] However, there is no reference from the dioxo,dithio-14-crown-4 family of molecules. Taking into account the fact that, in our systems, the cations are bonded to the oxygen atoms (see Table 2 and 3), the trends in the calculated selectivities could be compared with those of the dioxo-14-crown-4 systems. However, such a comparison is delicate because the ligand structure and experimental conditions can influence the selectivity.

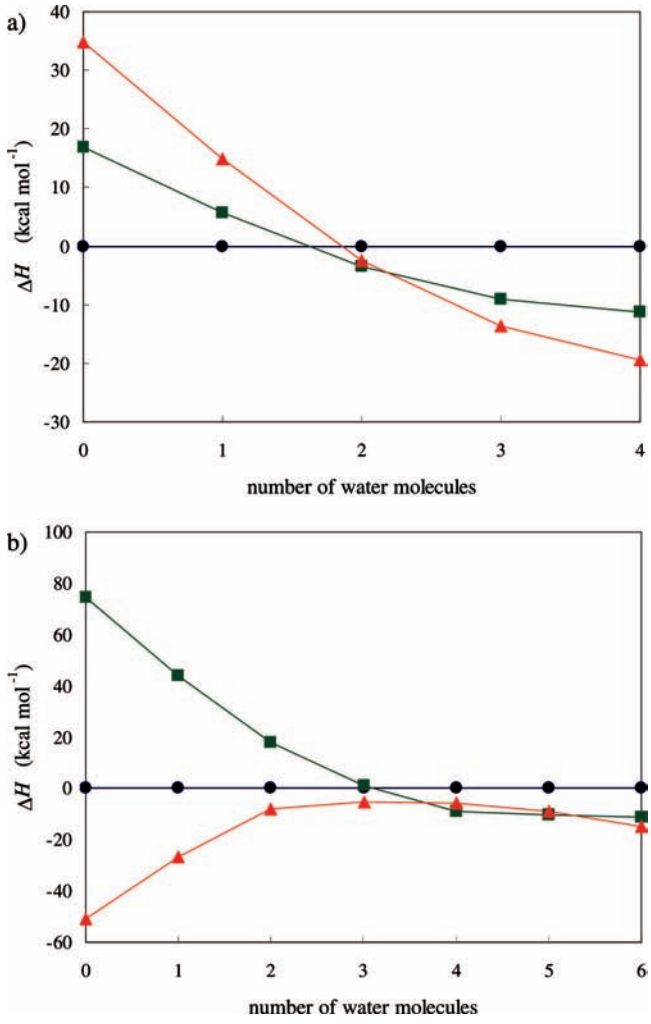

Figure 7. Reaction enthalpies for the exchange reactions of eq 2 (part a) and eq 3 (part b). The circles, squares, and triangles in part a (b) correspond to Li^+ (Mg^{2+}), Na^+ (Ca^{2+}), and K^+ (Zn^{2+}), respectively.

4. Conclusions

This theoretical DFT study on the interactions between a dioxadithia crown ether and mono- (Li^+, Na^+, K^+) and di- (Mg^{2+}, Ca^{2+}, Zn^{2+}) cations evidenced formation of two types of complexes with both groups of cations. In the first coordination mode, the cation is located in the crown. In the second coordination mode, the cation is located in a cage formed by the sugar cycles and the ester oxygen atoms. Except for the CE—K^+ system, the second type of complex is more stable with all of cations. Importantly, the dication complexes are, in general, more stable than those formed with monocations. The stability decreases with the period number; that is, the interaction energies for CE—Li^+ and CE—Mg^{2+} are more negative than those for CE—K^+ and CE—Ca^{2+}, respectively. The system interaction energy was decomposed into electrostatic, polarization, charge-transfer, exchange, and deformation contributions. The stabilizing contributions (ES, P, and CT) reflect the same trends as the interaction energy, whereas the destabilizing contributions show the opposite tendency. The polar effects (ES + P + CT) strongly favor formation of conformer 1, whereas steric repulsion (EX + DEF) does not show any regularity; the latter is due to an interplay between the EX and DEF energies. The total electrostatic energy, i.e., the sum of the first-order (ES) and second-order (P) contribution,s is a dominating term in the interaction energy. For the CE—X^+ complexes (X = Li, Na, or K), the CT energy is greater than or comparable to the ES and P energies. In the case of divalent cations, CT is always the least important stabilizing contribution.

The bond-order data are consistent with the results for the interaction energy and its components. The comparison of the CIBO and CBO results indicates an important ionic contribution to the bond-order indexes. The ionic contribution slightly improves the linear correlation of the BO values with the inter-reactant separation. A linear correlation with distance was also observed for the orbital energies (P + CT) of the CE—X^+ and CE—X^{2+} systems, respectively. No other energy components show such a correlation.

It is widely admitted that crown ether complexes are stabilized by electrostatic interactions (ion—distributed multipole). The results obtained in our work are in accordance with this simple model of interactions, because the EX and CT contributions cancel each other out to a great extent. However, the charge reorganization plots cannot be understood without taking into consideration the CT and EX contributions. The change in the electron density due to CT/EX is localized in the nearest neighborhood of the cations, whereas the P-induced change extends to a larger space.

In conclusion, the results obtained indicate that the stability of a crown ether ligand in cation complexation depends to a great extent on polar interactions; these interactions are more important than steric effects. This proposal explains the interpretive power of density-functional-based reactivity criteria[30] and shows the way toward engineering of efficient selective ligands.

It should be mentioned that the solvent effect is very important and strongly influences the selectivity. Indeed, the dioxadithia crown ether ligand bearing two myristoyl chains preserves its selectivity toward the zinc divalent cation when water molecules are taken into account, whereas its affinity toward magnesium and calcium is modified. The gas-phase selectivity sequence is completely reversed in the case of monovalent cations.

Acknowledgment. J.K. and B.K. acknowledge the financial support from the Ministry of Science and Higher Education, Poland (Project 1206/GDR/2007/03). The authors acknowledge computational grants MNiSW/SGI3700/UJ/161/2006, MNiSW/IBM_BC_HS21/UJ/060/2007, MNiSW/SGI4700/UJ/061/2007, and MEiN/SGI3700/ UJ/108/2006 from Cyfronet.

References and Notes

(1) Pedersen, C. J. *J. Am. Chem. Soc.* **1967**, *89*, 2495.
(2) Pedersen, C. J. *J. Am. Chem. Soc.* **1967**, *89*, 7017.
(3) Gokel, G. W.; Leevy, W. M.; Weber, M. E. *Chem. Rev.* **2004**, *104*, 2723.
(4) Badis, M.; Tomaszkiewicz, I.; Joly, J.-P.; Rogalska, E. *Langmuir* **2004**, *20*, 6259.
(5) Corvis, Y.; Korchowiec, B.; Korchowiec, J.; Badis, M.; Mironiuk-Puchalska, E.; Fokt, I.; Priebe, W.; Rogalska, E. *J. Phys. Chem. B* **2008**, *112*, 10935.
(6) Izatt, R. M.; Bradshaw, J. S.; Nielsen, S. A.; Lamb, J. D.; Christensen, J. J.; Sen, D. *Chem. Rev.* **1985**, *85*, 271.
(7) Izatt, R. M.; Pawlak, K.; Bradshaw, J. S.; Bruening, R. L. *Chem. Rev.* **1991**, *91*, 1721.
(8) Gokel, G. W. *Crown Ethers and Cryptands*; The Royal Society of Chemistry: London, 1991.
(9) Sannicolo, F.; Brenna, E.; Benincori, T.; Zotti, G.; Zecchin, S.; Schiavon, G.; Pilati, T. *Chem. Mater.* **1998**, *10*, 2167.
(10) Tokunaga, Y.; Nakamura, T.; Yoshioka, M.; Shimomura, Y. *Tetrahedron Lett.* **2006**, *47*, 5901.
(11) Mathias, L. J. *J. Macromol. Sci. Chem.* **1981**, *A15*, 853.
(12) Tran, C. D.; Zhang, W. *Anal. Chem.* **1990**, *62*, 830.
(13) Kuwahara, Y.; Nagata, H.; Nishi, H.; Tanaka, Y.; Kakehi, K. *Chromatographia* **2005**, *62*, 505.
(14) Chen, S.; Yuan, H.; Grinberg, N.; Dovletoglou, A.; Bicker, G. *J. Liq. Chromatogr. Relat. Technol.* **2003**, *26*, 425.

(15) Munoz, S.; Mallen, J.; Nakano, A.; Chen, Z.; Gay, I.; Echegoyen, L.; Gokel, G. W. *J. Am. Chem. Soc.* **1993**, *115*, 1705.
(16) Mazik, M.; Kuschel, M.; Sicking, W. *Org. Lett.* **2006**, *8*, 855.
(17) Cazacu, A.; Tong, C.; Van der Lee, A.; Fyles, T. M.; Barboiu, M. *J. Am. Chem. Soc.* **2006**, *128*, 9541.
(18) Pearson, R. G. *J. Am. Chem. Soc.* **1963**, *85*, 3533.
(19) Pearson, R. G. *Science* **1966**, *151*, 1721.
(20) Hancock, R. D.; Martell, A. E. *Chem. Rev.* **1989**, *89*, 1875.
(21) Bagatur'yants, A. A.; Freidzon, A. Y.; Alfimov, M. V.; Baerends, E. J.; Howard, J. A. K.; Kuz'mina, L. G. *J. Mol. Struct. (THEOCHEM)* **2002**, *588*, 55.
(22) Glendening, E. D.; Feller, D.; Thompson, M. A. *J. Am. Chem. Soc.* **1994**, *116*, 10657.
(23) Glendening, E. D.; Feller, D. *J. Am. Chem. Soc.* **1996**, *118*, 6052.
(24) Pingale, S. S.; Gadre, S. R.; Bartolotti, L. J. *J. Phys. Chem. A* **1998**, *102*, 9987.
(25) Feller, D.; Thompson, M. A.; Kendall, R. A. *J. Phys. Chem. A* **1997**, *101*, 7292.
(26) Hay, B. P.; Rustad, J. R.; Hostetler, C. J. *J. Am. Chem. Soc.* **1993**, *115*, 11158.
(27) Hataue, I.; Oishi, Y.; Kubota, M.; Fujimoto, H. *Tetrahedron* **1991**, *47*, 9317.
(28) Seidl, E. T.; Schaefer, H. F., III *J. Phys. Chem.* **1991**, *95*, 3589.
(29) Hori, K.; Yamada, H.; Yamabe, T. *Tetrahedron* **1983**, *39*, 67.
(30) Pullman, A.; Giessner-Prettre, C.; Kruglyak, Y. V. *Chem. Phys. Lett.* **1975**, *35*, 156.
(31) Brown, M. D.; Dyke, J. M.; Ferrante, F.; Levason, W.; Ogden, J. S.; Webster, M. *Chem. Eur. J.* **2006**, *12*, 2620.
(32) Vivas-Reyes, R.; De Proft, F.; Biesemans, M.; Willem, R.; Geerlings, P. *Eur. J. Inorg. Chem.* **2003**, 1315.
(33) Dreyfus, M.; Pullman, A. *Theor. Chim. Acta* **1970**, *19*, 20.
(34) Kollman, P. A.; Allen, L. C. *Theor. Chim. Acta* **1970**, *18*, 399.
(35) Morokuma, K. *J. Chem. Phys.* **1971**, *55*, 1236.
(36) Kitaura, K.; Morokuma, K *Int. J. Quantum Chem.* **1976**, *10*, 325.
(37) Ziegler, T.; Rauk, A. *Inorg. Chem.* **1979**, *18*, 1755.
(38) Sadlej, A. J. *Mol. Phys.* **1980**, *39*, 1249.
(39) Gutowski, M.; Piela, L. *Mol. Phys.* **1988**, *64*, 337.
(40) Glendening, E. D.; Streitwieser, A. *J. Chem. Phys.* **1994**, *100*, 2900.
(41) Glendening, E. D. *J. Am. Chem. Soc.* **1996**, *118*, 2473.
(42) Stevens, W. J.; Fink, W. H. *Chem. Phys. Lett.* **1987**, *139*, 15.
(43) Korchowiec, J.; Uchimaru, T. *J. Chem. Phys.* **2000**, *112*, 1623.
(44) Chen, W.; Gordon, M. S. *J. Phys. Chem.* **1996**, *100*, 14316.
(45) Frey, R. F.; Davidson, E. R. *J. Chem. Phys.* **1989**, *90*, 5555.
(46) Glendening, E. D. *J. Phys. Chem. A* **2005**, *109*, 11936.
(47) Hariharan, P. C.; Pople, J. A. *Theor. Chim. Acta* **1973**, *28*, 213.
(48) Morokuma, K. *Acc. Chem. Res.* **1977**, *10*, 294.
(49) Sokalski, W. A.; Roszak, S.; Hariharan, P. C.; Kaufman, J. J. *Int. J. Quantum Chem.* **1983**, *23*, 847.
(50) Sokalski, W. A.; Roszak, S.; Pecul, K. *Chem. Phys. Lett.* **1988**, *153*, 153.
(51) Sokalski, W. A.; Roszak, S. M. *J. Mol. Struct. (THEOCHEM)* **1991**, *80*, 387.
(52) White, J. C.; Davidson, E. R. *J. Chem. Phys.* **1990**, *93*, 8029.
(53) Frisch, M. J.; Trucks, G. W.; Schlegel, H. B.; Scuseria, G. E.; Robb, M. A.; Cheeseman, J. R.; Montgomery, J. A., Jr.; Vreven, T.; Kudin, K. N.; Burant, J. C.; Millam, J. M.; Iyengar, S. S.; Tomasi, J.; Barone, V.; Mennucci, B.; Cossi, M.; Scalmani, G.; Rega, N.; Petersson, G. A.; Nakatsuji, H.; Hada, M.; Ehara, M.; Toyota, K.; Fukuda, R.; Hasegawa, J.; Ishida, M.; Nakajima, T.; Honda, Y.; Kitao, O.; Nakai, H.; Klene, M.; Li, X.; Knox, J. E.; Hratchian, H. P.; Cross, J. B.; Bakken, V.; Adamo, C.; Jaramillo, J.; Gomperts, R.; Stratmann, R. E.; Yazyev, O.; Austin, A. J.; Cammi, R.; Pomelli, C.; Ochterski, J. W.; Ayala, P. Y.; Morokuma, K.; Voth, G. A.; Salvador, P.; Dannenberg, J. J.; Zakrzewski, V. G.; Dapprich, S.; Daniels, A. D.; Strain, M. C.; Farkas, O.; Malick, D. K.; Rabuck, A. D.; Raghavachari, K.; Foresman, J. B.; Ortiz, J. V.; Cui, Q.; Baboul, A. G.; Clifford, S.; Cioslowski, J.; Stefanov, B. B.; Liu, G.; Liashenko, A.; Piskorz, P.; Komaromi, I.; Martin, R. L.; Fox, D. J.; Keith, T.; Al-Laham, M. A.; Peng, C. Y.; Nanayakkara, A.; Challacombe, M.; Gill, P. M. W.; Johnson, B.; Chen, W.; Wong, M. W.; Gonzalez, C.; Pople, J. A. *Gaussian 03*; revision E.01; Gaussian, Inc.: Pittsburgh, PA, 2004.
(54) Schmidt, M. W.; Baldridge, K. K.; Boatz, J. A.; Elbert, S. T.; Gordon, M. S.; Jensen, J. H.; Koseki, S.; Matsunaga, N.; Nguyen, K. A.; Su, S.; Windus, T. L.; Dupuis, M.; Montgomery, J. A. *J. Comput. Chem.* **1993**, *14*, 1347.
(55) *GAMESS*, version March 24, 2007; Iowa State University: Ames, IA, 2003.
(56) Becke, A. D. *J. Chem. Phys.* **1993**, *98*, 5648.
(57) Becke, A. D. *Phys. Rev. A* **1988**, *38*, 3098.
(58) Lee, C.; Yang, W.; Parr, R. G. *Phys. Rev. B* **1988**, *37*, 785.
(59) Chirlian, L. E.; Francl, M. M. *J. Comput. Chem.* **1987**, *8*, 894.
(60) Korchowiec, J. *J. Mol. Struct. (THEOCHEM)* **2003**, *663*, 175.
(61) Korchowiec, J. *Int. J. Quantum Chem.* **2005**, *101*, 714.
(62) Korchowiec, J.; Chandra, A. K.; Uchimaru, T. *J. Mol. Struct. (THEOCHEM)* **2001**, *572*, 193.
(63) Mayer, I. *Chem. Phys. Lett.* **1983**, *97*, 270.
(64) Mayer, I. *Theor. Chim. Acta* **1985**, *67*, 315.
(65) Mayer, I. *Int. J. Quantum Chem.* **1986**, *29*, 477.
(66) Nalewajski, R. F.; Mrozek, J.; Michalak, A. *Int. J. Quantum Chem.* **1997**, *61*, 589.
(67) Mrozek, J.; Nalewajski, R. F.; Michalak, A. *Pol. J. Chem.* **1998**, *72*, 1779.
(68) Delbecq, F.; Ilavsky, D.; Nguyen Trong, A.; Lefour, J. M. *J. Am. Chem. Soc.* **1985**, *107*, 1623.
(69) Wong, M. W.; Pross, A.; Radom, L. *J. Am. Chem. Soc.* **1993**, *115*, 11050.
(70) Wong, M. W.; Pross, A.; Radom, L. *J. Am. Chem. Soc.* **1994**, *116*, 11938.
(71) Wong, M. W.; Pross, A.; Radom, L. *J. Am. Chem. Soc.* **1994**, *116*, 6284.
(72) Parr, R. G.; Pearson, R. G. *J. Am. Chem. Soc.* **1983**, *105*, 7512.
(73) Nalewajski, R. F. *J. Am. Chem. Soc.* **1984**, *106*, 944.
(74) Tedder, J. M. *Angew. Chem.* **1982**, *94*, 433.
(75) Tedder, J. M. *Tetrahedron* **1982**, *38*, 313.
(76) Tedder, J. M.; Walton, J. C. *Adv. Phys. Org. Chem.* **1978**, *16*, 51.
(77) Allouche, A. R. Gabedit 2.1.9. is a free graphical user interface for computational chemistry packages. It is available from http://gabedit.sourceforge.net.
(78) Christensen, J. J.; Eatough, D. J.; Izatt, R. M. *Chem. Rev.* **1974**, *74*, 351.
(79) Izatt, R. M.; Pawlak, K.; Bradshaw, J. S. *Chem. Rev.* **1995**, *95*, 2529.

JP8066052